Int. J. Heat Mass Transfer. Vol. 35, No. 12, pp. 3441–3450, 1992
Printed in Great Britain

0017–9310/92 $5.00+0.00

Gas turbine regenerators: A method for selecting the optimum plate-finned surface pair for minimum core volume

J. F. CAMPBELL
United States Navy Commander Submarine Force, U.S. Atlantic Fleet, Norfolk, Virginia, U.S.A.

and

W. M. ROHSENOW
Mechanical Engineering Department, Massachusetts Institute of Technology, Cambridge, MA 02139, U.S.A.

(*Received* 1 *January* 1991 *and in final form* 5 *November* 1991)

Abstract—A power law approximation for the Kays–London heat exchanger data as modified by Soland is used to derive a closed form solution for sizing counterflow regenerators. This solution is used to develop criteria for obtaining the minimum volume heat exchanger. These criteria are: (1) select a surface with minimum plate spacing for use on the cold side; (2) list other available surfaces with plate spacings approximately equal to the cold side plate spacing; (3) select from this list the surface with the minimum hydraulic diameter for use on the hot side.

1. INTRODUCTION

WHEN DESIGNING gas turbine regenerators for a given application, often the goals are to minimize volume and maximize heat transfer. In the past, sizing routines and procedures to select the optimum surface pair for counterflow plate-finned regenerators were iterative and complex. In this paper, a simplified method to solve these problems is presented.

Kays and London [1], hereafter denoted as KL, presented data for many plate-finned surfaces in terms of Colburn j-factors and friction factors, f. These factors referred to the exposed area, A_T, as a function of Reynolds number, based on the minimum free-flow area, A_c.

Soland *et al.* [2] developed a method to simplify comparison of different surfaces by converting the KL j and f factors reference area from A_T to the base plate area, A_b. Table 1 (equations (1) to (9)) shows Soland's definitions of the various quantities compared with those used by KL. Below is a pertinent excerpt from Soland [2]:

> The effect of the fins is included in the new j_n and f_n based on A_b. Further, the new Reynolds number, Re_n, is based on the open flow, A_F, *as though the fins were not present*. This requires that the metal conductivity of the fins, k, be specified in incorporating the effect of the fins into h_n.

To convert the KL data to Soland's basis, the following ratios obtained from equations (1) to (9) (see Table 1) and Fig. 1 are used

$$\frac{A_b}{A_T} = \frac{2XZ}{\beta V} = \frac{2}{\beta b} \tag{10}$$

where

$$\beta \equiv \frac{A_T}{V} \quad \left(\text{and } \beta_n \equiv \frac{A_b}{V} = \frac{2}{b}\right). \tag{11}$$

The other ratios are

$$\frac{A_F}{A_c} = \frac{XZb}{A_T r_h} = \frac{1}{\beta r_h} \tag{12}$$

$$\frac{G_n}{G_c} = \frac{A_c}{A_F} = \beta r_h \tag{13}$$

$$\frac{Re_n}{Re} = \frac{D_n G_n}{4 r_h G_c} = \frac{\beta b}{2} \tag{14}$$

$$\frac{f_n}{f} = \frac{A_F A_T G_c^2}{A_c A_b G_n^2} = \frac{b}{2\beta^2 r_h^3} \tag{15}$$

$$\frac{j_n}{j} = \frac{h_n}{h}\frac{G_c}{G_n} = \frac{\eta_0 b}{2 r_h}. \tag{16}$$

Figure 2 shows the two pairs of curves for a typical KL surface, namely their 3/16-11.1 plate-finned surface, Fig. 10.44 of reference [1].

Using the KL data as modified by Soland's method, an approximate closed-form solution for the counterflow sizing problem is derived in this paper. Then a sample calculation is performed and the effect of pressure drop is examined. Finally, a set of criteria for choosing the optimal surface pair is presented.

2. DERIVATION OF SIZING METHOD

Several preliminary steps are necessary before deriving the sizing method. The first is the key

NOMENCLATURE

a thickness of plate separating heat exchanger sides [m]
A_b heat transfer area of base surface which includes the effect of fins; equals length times heated perimeter [m^2]
A_c minimum free flow area [m^2]
A_F flow area ignoring any fins [m^2]
A_T total heat transfer area [m^2]
b plate spacing [m]
c specific heat [kJ kg^{-1} K^{-1}]
D_n nominal diameter; defined by equation (1b) [m]
f friction factor based on total area (A_T); defined by equation (4a)
f_n friction factor based on base area (A_b); defined by equation (4b)
g_0 conversion factor
G_c mass flux based on minimum free flow area; defined by equation (2a) [kg s^{-1} m^{-2}]
G_n mass flux based on free flow area (A_F); defined by equation (2b) [kg s^{-1} m^{-2}]
h heat transfer coefficient based on total area (A_T); defined by equation (5a) [W m^{-2} K^{-1}]
h_n heat transfer coefficient based on base area (A_b); defined by equation (5b) [W m^{-2} K^{-1}]
j Colburn j-factor based on total area (A_T); defined by equation (6a)
j_n Colburn j-factor based on base area (A_b); defined by equation (6b)
k thermal conductivity of heat exchanger metal [W m^{-1} K^{-1}]
K_f y-axis intercept of 'new best-fit' line with slope $= -s$; defined by equation (17b)
K_j y-axis intercept of 'new best-fit' line with slope $= -s$; defined by equation (17a)
L_f fin length from root to center ($=b/2$) [m]
m component of fin efficiency (n_f); defined by equation (9)
p pressure [Pa]
P component of core volume formula derived according to pressure drop considerations; defined by equation (26) [m^{3-2s}]
Pr Prandtl number
q heat transfer rate [W]
q/A heat flux [W m^{-2}]
Q component of core volume formula derived according to heat transfer considerations; defined by equation (34) [m^{2s+1}]
r correlation coefficient
r_h hydraulic radius; defined by equation (1a) [m]
R gas constant [J kmol^{-1} K^{-1}]
Re Reynolds number based on minimum free flow area (A_c); defined by equation (3a)
Re_n Reynolds number based on free flow area (A_F); defined by equation (3b)
s average slope of all best-fit lines through j_n and f_n vs Re_n data points
T temperature [K]
U overall heat transfer coefficient [W m^{-2} K^{-1}]
V volume [m^3]
W turbine work [N m]
X heat exchanger width [m]
XY heat exchanger frontal area [m^2]
Y heat exchanger height [m]
Z heat exchanger length [m].

Greek symbols

α ratio of total area on one side of the heat exchanger to total volume of the heat exchanger; defined by equation (18) [m^{-1}]
β ratio of total heat transfer area on one side to the volume on that side [m^{-1}]
δ fin thickness [m]
δT temperature difference; as shown in Fig. 4 [K]
ΔT temperature difference; as shown in Fig. 4 [K]
Δp friction pressure drop [Pa]
γ $(c_p - c_v)/c_v$
η_f fin efficiency; defined by equation (8)
η_0 total surface temperature effectiveness; defined by equation (7)
η_T turbine efficiency
μ viscosity [Pa s]
ρ density [kg m^{-3}]
σ ratio of free flow area to frontal area; defined by equation (19)
ω mass flow rate [kg s^{-1}].

Subscripts

n denotes a parameter modified according to Soland's method, [2]
1,2 indicates different sides of heat exchanger
h,c indicates hot or cold side of the heat exchanger.

Table 1. Definitions

Quantity	Kays and London [1]		Soland [2]	
Hydraulic diameter or radius	$r_h \equiv \frac{A_c Z}{A_T}$	(1a)	$D_n \equiv \frac{4A_F Z}{A_h} = \frac{4V}{A_h}$	(1b)
Mass flux	$G_c \equiv \frac{\omega}{A_c}$	(2a)	$G_n \equiv \frac{\omega}{A_F}$	(2b)
Reynolds number	$Re \equiv \frac{4G_c r_h}{\mu}$	(3a)	$Re_n \equiv \frac{G_n D_n}{\mu}$	(3b)
Friction factor	$f \equiv \frac{(\Delta p) r_h (2\rho g_0)}{ZG_c^2}$	(4a)	$f_n \equiv \frac{(\Delta p) D_n (2\rho g_0)}{4ZG_n^2}$	(4b)
Heat transfer coefficient	$h \equiv \frac{q/\eta_0 A_T}{\Delta T}$	(5a)	$h_n \equiv \frac{q/A_h}{\Delta T}$	(5b)
Colburn j-factor	$j \equiv \frac{h}{G_c c_p}(Pr)^{2/3}$	(6a)	$j_n \equiv \frac{h_n}{G_n c_p}(Pr)^{2/3}$	(6b)

The efficiencies are defined by equations (7), (8) and (9).

$$\eta_0 \equiv 1 - \frac{XY}{A_T}(1-\eta_f) \tag{7}$$

$$\eta_f \equiv \frac{\tanh(mL_f)}{mL_f} \tag{8}$$

$$m \equiv \sqrt{\left(\frac{2}{\delta}\frac{h}{k}\right)}. \tag{9}$$

approximation of fitting straight lines through the modified KL data points, j_n and f_n vs Re_n. These lines have the functional relationships

$$j_n = K_j Re_n^{-s} \tag{17a}$$

and

$$f_n = K_f Re_n^{-s}. \tag{17b}$$

The values for s, K_j, and K_f are determined using a linear regression routine. A 'best-fit' line is found for each surface's j_n and f_n vs Re_n data points. Table 2 lists the slopes of these best-fit lines with the associated correlation coefficient, r (defined in [3]), for each of the 26 KL surfaces examined in this study. Generally, the j_n and f_n vs Re_n data are well represented by straight lines as evidenced by the fact that all correlation coefficients are greater than 0.93. By averaging the slopes from Table 2, the value to be used for s in equations (17a) and (17b) is found to be 0.46.

With s thus determined, the j_n and f_n vs Re_n data for each surface are revisited. This time, 'new best-fit' lines are determined but the slopes of the lines are fixed at s equal to 0.46 for all surfaces. Figure 3 is a plot of this kind for the typical KL surface, 3/16-11.1. The constants, K_j and K_f, for surface 3/16-11.1 are shown graphically on Fig. 3. The constants of the new best-fit lines for the other surfaces are listed in Table 2. Appendix A of reference [4] contains graphs similar to Fig. 3 which also show the average error for each surface's j_n and f_n data set. For the 26 surfaces in Table 2, the average error never exceeded 10% and for most surfaces is near 3% or 4%.

Next, define two heat exchanger core geometrical parameters, α_n and σ_n

$$\alpha_{n1} \equiv \frac{A_{b1}}{V_T} = \frac{2}{b_1 + b_2 + 2a} \simeq \frac{2}{b_1 + b_2} \tag{18a}$$

$$\alpha_{n2} \equiv \frac{A_{b2}}{V_T} \simeq \frac{2}{b_1 + b_2} = \alpha_1. \tag{18b}$$

Note that in equations (18a) and (18b) the heat transfer resistance of the plate (thickness = a) separating the two sides of the heat exchanger is considered negligible and therefore the '$2a$' term is dropped. The other geometrical parameter is

$$\sigma_{n1} \equiv \frac{A_{F1}}{XY} = \frac{b_1}{b_1 + b_2} \tag{19a}$$

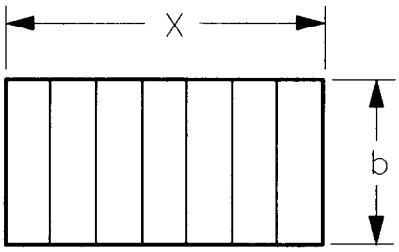

$A_F = Xb$ $\quad D_n = 4\frac{V}{A_b} = 4\frac{XZb}{2XZ} = 2b$

$A_b = 2XZ$ $\quad G_n = \frac{\omega}{A_F} = \frac{\omega}{Xb}$

$V = XZb$

FIG. 1. Sample calculation of nominal diameter and mass flux for rectangular flow passage.

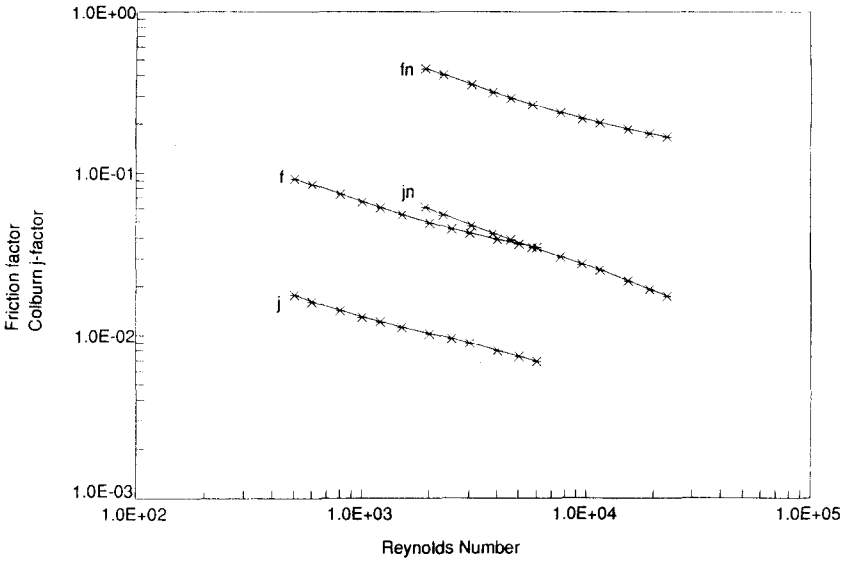

FIG. 2. j and f vs Re; j_n and f_n vs Re_n for surface 3/16–11.1.

$$\sigma_{n2} \equiv \frac{A_{F2}}{XY} = \frac{b_2}{b_1 + b_2}. \tag{19b}$$

The mass flux, G_n and Reynolds number, Re_n can be written in terms of these geometrical parameters as

$$G_{n1} = \frac{\omega_1}{A_{F1}} = \frac{\omega_1}{\sigma_{n1} XY} = \frac{\omega_1}{XY}(1 + b_2/b_1) \tag{20}$$

$$Re_{n1} = \frac{G_{n1} D_{n1}}{\mu_1} = \frac{\omega_1}{\sigma_{n1} XY} \frac{2b_1}{\mu_1} = \frac{\omega_1}{XY} \frac{2b_1}{\mu_1}(1 + b_2/b_1) \tag{21}$$

with similar results for G_{n2} and Re_{n2}.

The remaining preliminary step is to specify the operating conditions for which the regenerator will be

Table 2. Surfaces

Surface name from KL [1]	Name used in paper	Hydraulic diameter, $4r_h$ (m)	Plate spacing, b (m^{-1})	j_n			f_n		
				Slope	r	K_j	Slope	r	K_f
1/10-19.74	S27	1.22	1.29	−0.440	0.995	0.656	−0.457	0.977	3.919
1/10-19.35	S29	1.40	1.91	−0.484	0.999	1.069	−0.522	0.992	5.265
1/9-24.12	S28	1.21	1.91	−0.434	0.993	1.312	−0.493	0.988	8.737
3/8(b)-11.1	L19	3.084	6.35	−0.486	0.999	1.746	−0.376	0.980	11.561
3/4-11.1	L21	3.084	6.35	−0.484	0.999	1.396	−0.454	0.982	8.060
3/8-11.1	L18	3.084	6.35	−0.506	0.999	1.773	−0.388	0.982	11.806
3/16-11.1	L15	3.084	6.35	−0.497	0.999	1.872	−0.395	0.995	14.766
11.1	P04	3.084	6.35	−0.395	0.983	0.932	−0.441	0.960	4.141
1/2-11.1	L20	3.084	6.35	−0.473	0.997	1.514	−0.375	0.971	9.436
3/4(b)-11.1	L22	3.084	6.35	−0.459	0.999	1.380	−0.429	0.982	8.068
1/8-16.12T	S31	1.57	7.98	−0.607	0.998	4.440	−0.378	0.965	52.575
14.77	P06	2.59	8.38	−0.503	0.996	1.615	−0.493	0.972	10.369
30.33T	P10	1.222	8.76	−0.790	0.999	4.314	−0.807	0.991	29.905
1/6-12.18D	S30	2.70	8.97	−0.641	0.999	2.656	−0.498	0.985	18.694
6.2	P02	5.54	10.29	−0.306	0.938	0.686	−0.371	0.943	3.092
17.8-3/8W	W27	2.12	10.49	−0.612	0.999	4.046	−0.435	0.999	45.642
11.44-3/8W	W26	3.23	10.49	−0.549	0.999	3.014	−0.391	1.000	34.107
1/8-15.2	S25	2.65	10.55	−0.489	0.999	3.575	−0.335	0.969	47.617
15.08	P07	2.67	10.62	−0.621	0.986	1.447	−0.640	0.969	7.032
5.3	P01	6.15	11.94	−0.403	0.996	0.987	−0.458	0.972	3.226
11.11(a)	P05	3.52	12.19	−0.396	0.936	2.046	−0.516	0.959	8.833
3/32-12.22	S24	3.41	12.3	−0.584	0.999	2.899	−0.385	0.980	41.038
3.97	P14	8.59	19.05	−0.331	0.989	1.274	−0.260	0.969	5.607
2.0	P12	14.45	19.05	−0.313	0.997	0.790	−0.212	0.976	2.648
3.01	P13	10.82	19.05	−0.339	0.987	1.007	−0.264	0.968	4.448
9.03	P03	4.64	20.90	−0.537	0.987	1.625	−0.418	0.946	12.057

K_j and K_f are determined for the average slope equal to −0.46.

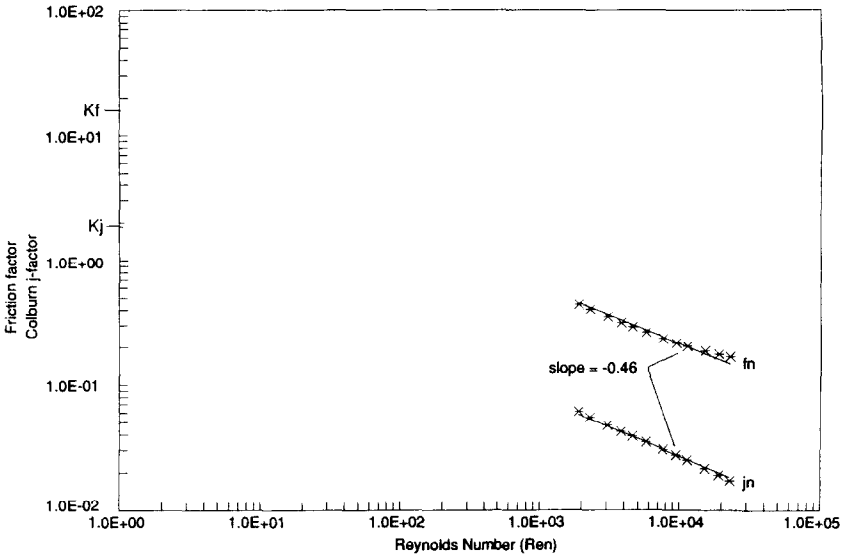

FIG. 3. Surface 3/16–11.1 'New Best-Fit' Line (slope = −0.46).

sized. The operating conditions for the examples in this study are shown in Fig. 4.

Having completed the above preliminary steps, it is now possible to derive the approximate closed-form formula for sizing a counterflow regenerator. The derivation consists of three steps. First, the heat exchanger core size (X, Y, and Z) is found as a function of the allowable pressure drop. Step two finds the core size based on heat transfer considerations. In step three, the equations resulting from steps one and two are solved simultaneously to yield the formula for core volume.

STEP 1. From equation (4b), the pressure drop equation can be written as

$$\frac{\Delta p_1}{p_1} = \frac{4 f_{n1} Z_1 G_{n1}^2}{p_1 (2\rho_1 g_0) D_{n1}}. \tag{22}$$

Substitute for f_n using equation (17b), use $Z_1 = Z_2 = Z$ for counterflow arrangement and substitute for $2b_1 = D_n$ from Fig. 1

$$\frac{\Delta p_1}{p_1} = \frac{4 K_{f1} Re_{n1}^{-s}}{\rho_1 p_1} \frac{Z}{2b_1} \frac{G_{n1}^2}{2g_0}. \tag{23}$$

Substitute for G_n from (20) and Re_n from equation (21) and rearrange

$$\frac{\Delta p_1}{p_1} = \frac{2 K_{f1} Z \mu_1^s}{p_1 \rho_1 g_0 (2b_1)^{s+1}} \left(\frac{\omega}{XY} (1 + b_2/b_1) \right)^{2-s}. \tag{24a}$$

Similarly

$$\frac{\Delta p_2}{p_2} = \frac{2 K_{f2} Z \mu_2^s}{p_2 \rho_2 g_0 (2b_2)^{s+1}} \left(\frac{\omega}{XY} (1 + b_1/b_2) \right)^{2-s}. \tag{24b}$$

Combining equations (24a) and (24b) and letting $\mu_1 = \mu_2 = \mu$, then

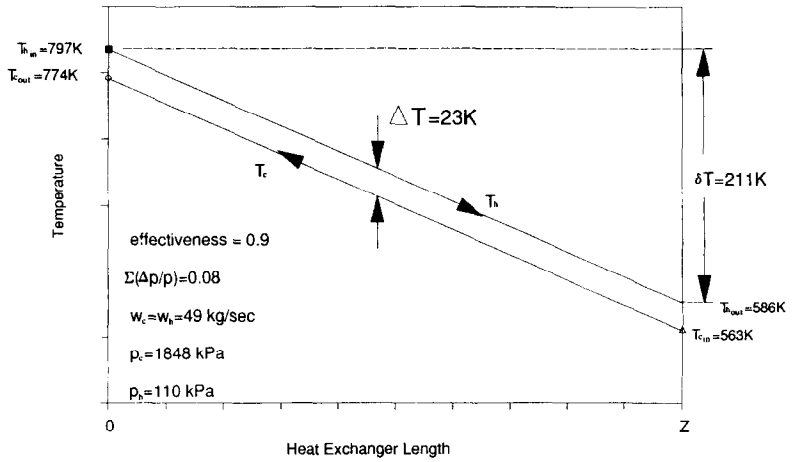

FIG. 4. Operating conditions.

$$\Sigma\frac{\Delta p}{p}=\frac{\Delta p_1}{p_1}+\frac{\Delta p_2}{p_2}=\frac{2Z\mu^s}{g_0}\left(\frac{\omega}{XY}\right)^{2-s}\times\left(\frac{K_{f1}(1+b_2/b_1)^{2-s}}{p_1\rho_1(2b_1)^{s+1}}+\frac{K_{f2}(1+b_1/b_2)^{2-s}}{p_2\rho_2(2b_2)^{s+1}}\right). \quad (25)$$

Define the heat exchanger size in terms of pressure drop as P

$$P\equiv\frac{(XY)^{2-s}}{Z}. \quad (26)$$

Substituting $\rho=RT/p$ from the ideal gas relationship, then from equations (25) and (26)

$$P=\frac{2RT_1\mu^s\omega^{2-s}}{\Sigma\left(\frac{\Delta p}{p}\right)g_0p_1^2}\frac{K_{f1}}{(2b_1)^{s+1}}(1+b_2/b_1)^{2-s}\times\left[1+\frac{K_{f2}}{K_{f1}}\left(\frac{p_1}{p_2}\right)^2\frac{T_2}{T_1}\left(\frac{b_1}{b_2}\right)^3\right]. \quad (27)$$

STEP 2. The heat transfer rate equation from reference [5] is

$$q=UA_h(\Delta T) \quad (28)$$

where

$$\frac{1}{UA_h}=\left(\frac{1}{h_nA_h}\right)_1+\left(\frac{1}{h_nA_h}\right)_2. \quad (29)$$

From equation (6b)

$$h_{n1}=j_{n1}\frac{c_{p1}G_{n1}}{(Pr_1)^{2/3}}. \quad (30)$$

Substitute for j_{n1} using equation (17a)

$$h_{n1}=K_{j1}\frac{c_{p1}}{(Pr_1)^{2/3}}Re_{n1}^{-s}G_{n1}. \quad (31)$$

Substitute for G_n from equation (20), Re_n from equation (21), let $Pr_1=Pr_2=Pr$, $c_{p1}=c_{p2}=c_p$ and rearrange

$$\frac{1}{h_{n1}}=\frac{Pr^{2/3}}{c_p}\left(\frac{XY}{\omega}\right)^{1-s}\frac{1}{\mu^s}\left[\frac{1}{K_{j1}}\left(\frac{b_1}{b_1+b_2}\right)^{1-s}(2b_1)^s\right]. \quad (32a)$$

Similarly,

$$\frac{1}{h_{n2}}=\frac{Pr^{2/3}}{c_p}\left(\frac{XY}{\omega}\right)^{1-s}\frac{1}{\mu^s}\left[\frac{1}{K_{j2}}\left(\frac{b_2}{b_1+b_2}\right)^{1-s}(2b_2)^s\right]. \quad (32b)$$

Combining equations (32a) and (32b) with equations (28) and (29) and using

$$A_h=\alpha_nXYZ=\frac{2XYZ}{(b_1+b_2)}$$

from equation (18), then

$$\frac{\Delta T}{q}=\frac{(b_1+b_2)Pr^{2/3}}{2(XY)^sZc_p\omega^{1-s}\mu^s}\left[\frac{1}{K_{j1}}\left(\frac{b_1}{b_1+b_2}\right)^{1-s}(2b_1)^s+\frac{1}{K_{j2}}\left(\frac{b_2}{b_1+b_2}\right)^{1-s}(2b_2)^s\right]. \quad (33)$$

Define the heat exchanger size in terms of heat transfer as Q

$$Q\equiv(XY)^sZ. \quad (34)$$

Then substituting equation (33) into equation (34) and rearranging

$$Q=\frac{(b_1+b_2)qPr^{2/3}}{2(\Delta T)c_p\omega^{1-s}\mu^s}\left[\left(\frac{b_1}{b_1+b_2}\right)^{1-s}\frac{(2b_1)^s}{K_{j1}}+\left(\frac{b_2}{b_1+b_2}\right)^{1-s}\frac{(2b_2)^s}{K_{j2}}\right]. \quad (35)$$

Make the substitution $q=\omega c_p\delta T$ (where the relationship between ΔT and δT is shown in Fig. 4) and rearrange

$$Q=\left(\frac{\delta T}{\Delta T}\frac{\omega^sPr^{2/3}}{\mu^s}\right)\left(\frac{b_1^{s+1}}{2^{1-s}K_{j1}}\right)\left(1+\frac{b_2}{b_1}\right)^s\left(1+\frac{K_{j1}}{K_{j2}}\frac{b_2}{b_1}\right). \quad (36)$$

STEP 3. The definitions for P, equation (26), and Q, equation (34), provide two equations for the two unknowns, (XY) and Z. Solving these simultaneously, the closed-form solution for the heat exchanger core volume is

$$XY=(PQ)^{1/2} \quad (37a)$$

$$Z=P^{-s/2}Q^{1-s/2} \quad (37b)$$

$$V=P^{(1-s)/2}Q^{(3-s)/2}. \quad (37c)$$

3. EXAMPLE CALCULATION

For simplicity, this study is made for one set of operating conditions with equal flow rates and constant fluid properties on both sides as shown in Fig. 4. The calculated heat exchanger volumes are not precise; however, with variable properties and flow rates ratios of 0.85 to 1.0 the general trend of the results should be essentially the same.

Using the calculation method described previously, heat exchanger volumes are determined by putting each surface on the cold side and then pairing it with every other surface on the hot side. Appendix B of references [4] contains tables of data showing the volumes of heat exchangers with each of the 26 surfaces in Table 2 on the cold side. The resulting volumes for the typical surface 3/16-11.1 on the cold side are plotted in Fig. 5 with the ratio of plate spacing, b_h/b_c, as the abscissa and each point labelled with its hydraulic diameter, $4r_h$. Since there is no geometric similarity, distinct curves cannot be expected; however, the shaded regions group ranges of hydraulic diameters as shown. As another example,

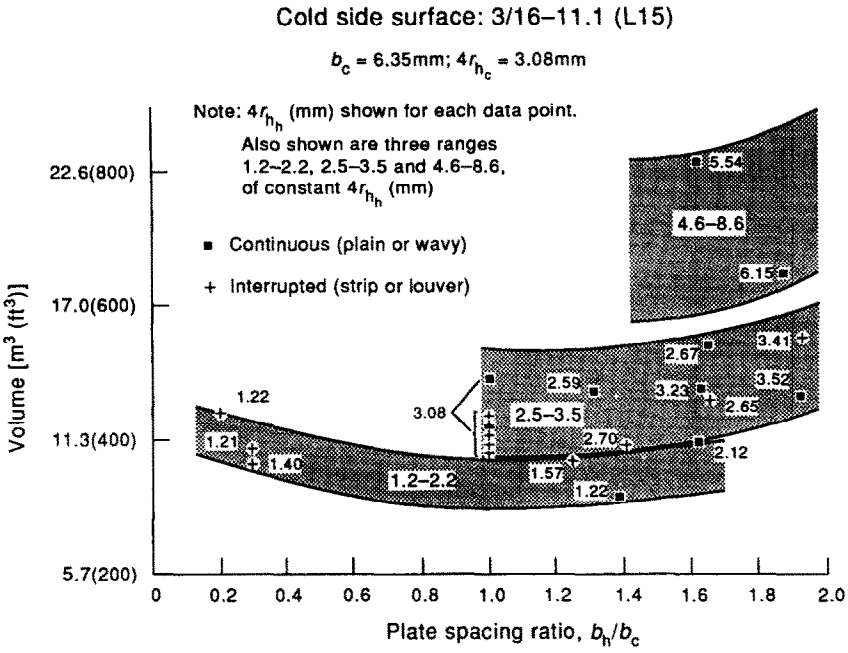

FIG. 5. Volume vs plate spacing ratio and hydraulic diameter. Cold side surface: 3/16–11.1 (L15).

select the smallest plate spacing, 1.29 m^{-3}, surface 1/10-19.74 (S27), for the cold side and put all of the other surfaces on the hot side. The results are plotted as Fig. 6. In one more example, a much larger plate spacing, 10.49 m^{-3}, wavy finned surface 17.8-3/8W (W27), is placed on the cold side and the other surfaces are put on the hot side. These results are plotted in Fig. 7.

In Fig. 6, the solid square point at plate spacing ratio of 8.2 labelled with $4r_h = 2.12$ m^{-3} represents the exchanger with the narrow surface (S27) on the cold side and the wider surface (W27) on the hot side. This combination results in a regenerator volume of approximately 5.7 m^3. In Fig. 7, the plus point at plate spacing ratio of 0.012 labelled with $4r_h = 1.22$ m^{-3} represents the exchanger with the wide surface (W27)

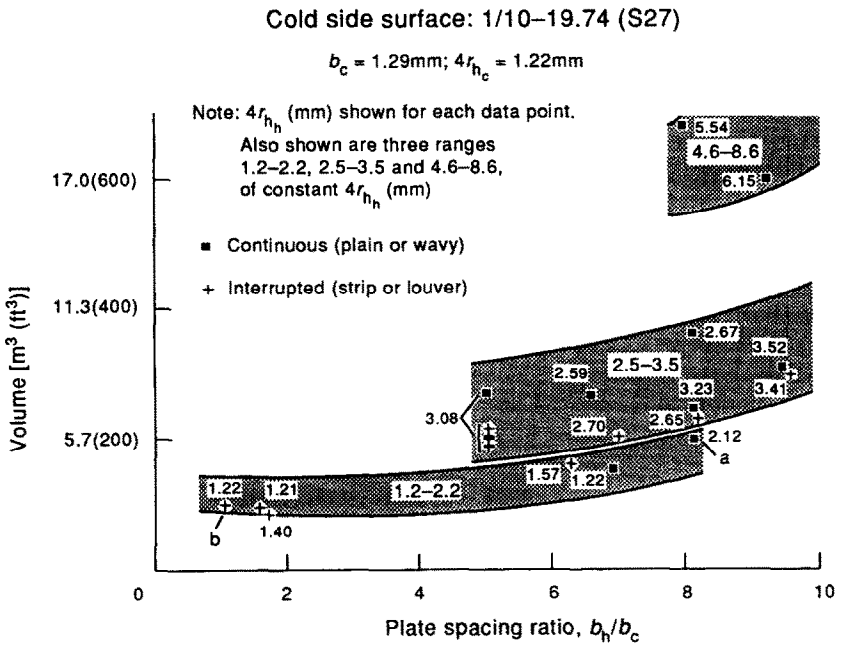

FIG. 6. Volume vs plate spacing ratio and hydraulic diameter. Cold side surface: 1/10–19.74 (S27).

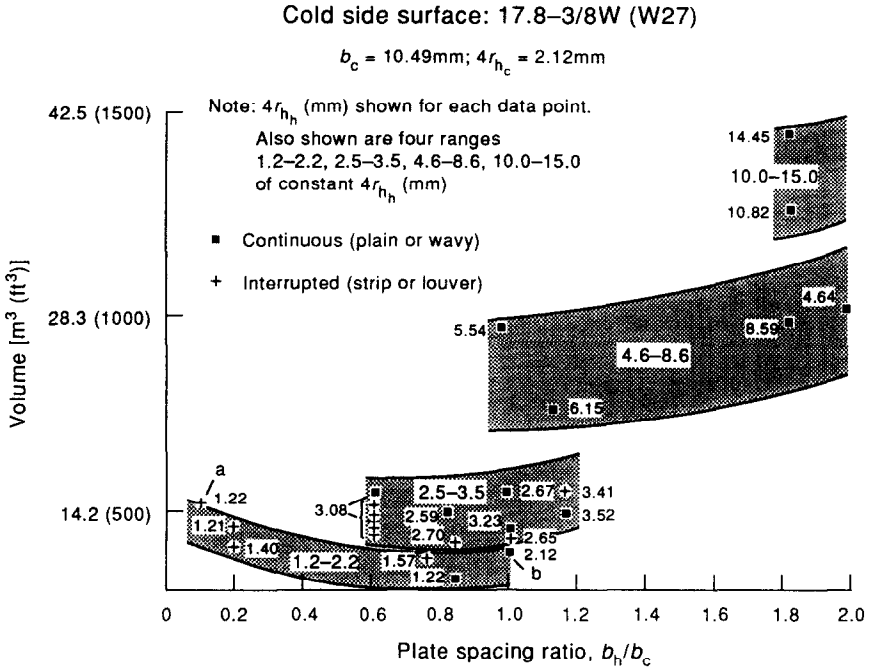

FIG. 7. Volume vs plate spacing ratio and hydraulic diameter. Cold side surface: 17.8–3/W (W27).

on the cold side and the narrow surface (S27) on the hot side. This pair yields a volume of about 14.7 m^3. These points are labelled as 'a' in Figs 6 and 7. This suggests that if different surfaces are used on the two sides then the narrow plate spacing should be placed on the cold side. Results similar to these were obtained for the other surfaces examined in reference [4].

Furthermore, in Fig. 6 the plus point with $4r_h = 1.22$ m^{-3} labelled 'b' represents the exchanger with the narrow surface (S27) on both sides. This exchanger has a volume approximately equal to 2.8 m^3. In Fig. 7, the solid square point with $4r_h = 2.12$ m^{-3} labelled 'b' represents the exchanger with wide surface (W27) on both sides and volume of 11.6 m^3. These results are summarized in Table 3.

It is not surprising to find smaller volumes accompanying smaller hydraulic diameters on the hot side. What is surprising is that the minimum volumes occur at plate spacing ratios of b_h/b_c in a range from 0.8 to 1.8. In gas turbines that have been constructed, it is quite common to find larger spacing ratios, b_h/b_c, of approximately five. Such a selection should be motivated by the desire for readily cleaned hot side passages but not by any necessity to re-distribute pressure drops.

Table 3. Volumes

Figure	Cold side	Hot side	Volume (m^3)
Fig. 6, point 'b'	S27	S27	2.8
Fig. 6, point 'a'	S27	W27	5.7
Fig. 7, point 'b'	W27	W27	11.6
Fig. 7, point 'a'	W27	S27	14.7

Of the 600 surface pairs examined in reference [4], using the operating conditions shown on Fig. 4, the combination of surface 1/9-24.12 on the cold side with surface 1/10-19.35 on the hot side results in the minimum heat exchanger core volume.

4. THE EFFECT OF PRESSURE DROP; $\Sigma(\Delta p/p)$

The expression for turbine work is

$$W = \omega \eta_T c_p T_h \left[1 - \left(\frac{p_c + \Delta p_c}{p_h - \Delta p_h}\right)\right]. \tag{38}$$

When expanded in a power series with $\Delta p/p$ small, the result is

$$\frac{W}{\omega \eta_T c_p T_h} = 1 - \left(\frac{p_c}{p_h}\right)^{\gamma}\left(1 + \gamma\frac{\Delta p_h}{p_h} + \gamma\frac{\Delta p_c}{p_c} + \cdots\right) \tag{39}$$

which shows that the loss in turbine work is proportional to the sum of $\Delta p/p$ on the sides

$$\frac{\Delta W}{W_s} = \frac{\gamma\Sigma\left(\frac{\Delta p}{p}\right)}{1 - \left(\frac{p_h}{p_c}\right)^{\gamma}}. \tag{40}$$

It does not matter how $\Delta p/p$ is distributed between the two sides; it is $\Sigma(\Delta p/p)$ that determines the loss in

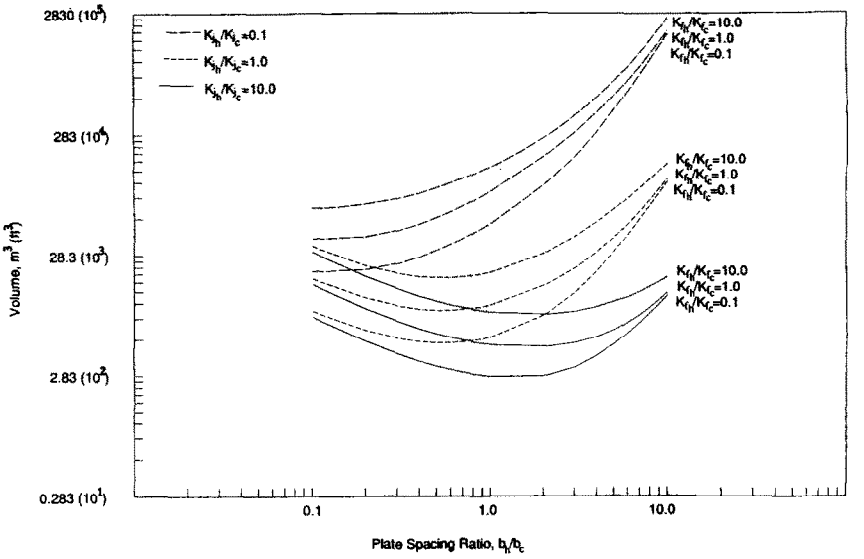

FIG. 8. Volume $= f\ (b_h/b_c,\ K_{jh}/K_{jc},\ K_{fh}/K_{fc})$.

turbine work for fixed compressor work and pressure ratio.

In high effectiveness counterflow heat exchangers, the ratio of the pressure drops on the two sides are fixed by the flow rates, densities, and free flow areas. The free flow areas are approximated by the plate spacings. The passage lengths are the same. Neglecting entrance and exit losses,

$$\Delta p = 4f\frac{Z}{4r_h}\frac{(\omega/A_c)^2}{2g_c\rho}\cdots. \tag{41}$$

For plate-fin surfaces, the friction factor varies approximately as

$$f \approx \left(\frac{\omega}{A_c}\frac{4r_h}{\mu}\right)^{-0.4}\cdots. \tag{42}$$

For the same Z

$$\frac{\Delta p_c}{\Delta p_h} = \left(\frac{\omega_c}{\omega_h}\right)^{1.6}\left(\frac{A_{c,h}}{A_{c,c}}\right)^{1.6}\left(\frac{r_{h,h}}{r_{h,c}}\right)^{1.4}\frac{\rho_h}{\rho_c}\cdots. \tag{43}$$

The relative flatness of the volume curves in Figs 5, 6 and 7 suggests using the same surfaces on both sides. Then for the case of perfect gases with equal flow rates

$$\frac{\Delta p_c}{\Delta p_h} = \frac{\rho_h}{\rho_c} = \left(\frac{p_h}{p_c}\right)\left(\frac{T_{m,c}}{T_{m,h}}\right)\cdots \tag{44}$$

and

$$\frac{\Delta p_c/p_c}{\Delta p_h/p_h} = \left(\frac{p_h}{p_c}\right)^2\left(\frac{T_{m,c}}{T_{m,h}}\right). \tag{45}$$

Since $T_{m,c}/T_{m,h} = 0.966$ and the pressure ratio from Fig. 4 is $p_c/p_h = 16.7$, then

$$\frac{\Delta p_c}{\Delta p_h} \approx 0.058 \quad \text{and} \quad \frac{\Delta p_c/p_c}{\Delta p_h/p_h} \approx 0.0035. \tag{46}$$

This shows that Δp and $(\Delta p/p)$ ratios will be orders of magnitude from unity in order to obtain minimum volume exchangers. This should not be of great concern since, according to equations (39) and (40), it does not matter how $(\Delta p/p)$ is distributed because the loss in cycle net work is determined only by the total $\Sigma(\Delta p/p)$.

5. CONCLUSIONS

Gas turbine regenerator designs have traditionally favored large plate spacing ratios, presumably to balance cold and hot side pressure drops. In light of equations (39) and (40), this is not necessary from turbine work loss or cycle efficiency considerations. Since the volume curves of Figs 5, 6 and 7 are relatively flat for low hydraulic diameters, the plate spacing ratio can vary considerably without substantially affecting the volume.

Examination of equations (27), (36) and (37) reveals that for a given set of operating conditions (such as those in Fig. 4), if the surface on side one is the cold side then the volume of the heat exchanger is such that

$$V = f\left[\frac{b_h}{b_c}, \frac{K_{fh}}{K_{fc}}, \left(\frac{K_{jh}}{K_{jc}}\right)^{-1}, \text{operating conditions}\right]. \tag{47}$$

Figure 8 is plot of volume vs plate spacing ratio, b_h/b_c, with lines of constant K_{fh}/K_{fc} and K_{jh}/K_{jc} when the typical surface 3/16-11.1 is on the cold side and the operating conditions are those shown in Fig. 4. From this figure it is apparent that the volume is minimized when K_{fh}/K_{fc} is minimized, K_{jh}/K_{jc} is maximized, and b_h/b_c is approximately one. A pair of 'ideally designed'

surfaces would meet these criteria and result in the minimum core volume.

This study suggests that, commensurate with fouling and cleaning needs, the smallest hydraulic diameter should be selected for the cold side and surfaces with small hydraulic diameters that result in plate spacing ratios close to unity should be selected for the hot side to obtain the minimum heat exchanger core volume. This can be developed into a set of criteria for selecting the pair of surfaces for minimum volume. For given operating conditions, volume will be minimized by following the steps below.

(1) Choose the narrowest plate spacing for the cold side (side one) based on constraints such as fabrication difficulty fouling.
(2) List all other available surfaces with plate spacings nearly equal to the cold side plate spacing (i.e. $b_h/b_c \cong 1.0$).
(3) Select from this list the surface with the minimum hydraulic diameter for use on the hot side.

REFERENCES

1. W. M. Kays and A. L. London, *Compact Heat Exchangers*, 3rd Ed, McGraw Hill, New York (1984).
2. J. G. Soland, W. M. Mack, Jr. and W. M. Rohsenow, Performance ranking of plate-fin heat exchangers, *ASME J. Heat Transfer* **100**, 514–519 (1978).
3. W. H. Bever, *CRC Standard Mathematical Tables*. 27th Ed, CRC Press, Boca Raton, FL (1984).
4. J. F. Campbell, Jr., Gas turbine regenerators: a method for selecting the optimum plate-finned surface pair for minimum core volume. Ocean Engineering Thesis, Massachusetts Institute of Technology, Cambridge, MA (1989).
5. W. M. Rohsenow and H. Choi, *Heat, Mass and Momentum Transfer*, Prentice-Hall, Englewood Cliffs, NJ (1961).